

Supplemental information

**Dual pancreatic adrenergic and dopaminergic
signaling as a therapeutic target of bromocriptine**

Despoina Aslanoglou, Suzanne Bertera, Laura Friggeri, Marta Sánchez-Soto, Jeongkyung Lee, Xiangning Xue, Ryan W. Logan, J. Robert Lane, Vijay K. Yechoor, Peter J. McCormick, Jens Meiler, R. Benjamin Free, David R. Sibley, Rita Bottino, and Zachary Freyberg

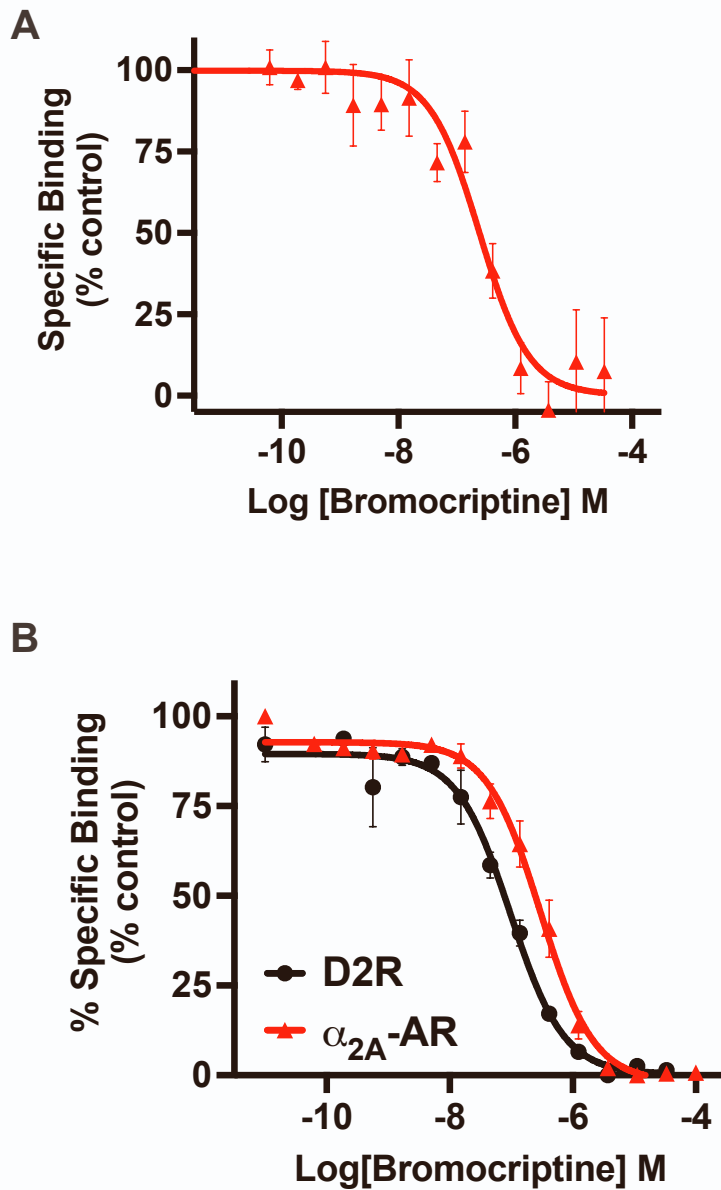


Figure S1. Bromocriptine binds directly to D2R and α_{2A} -AR, related to Figure 1. (A) Radioligand competition with bromocriptine at endogenously expressed α_{2A} -AR in INS-1E cells. Competition binding curve of the α_{2A} -AR antagonist [3 H]-RX821002 versus increasing concentrations of bromocriptine showed binding of bromocriptine to endogenous α_{2A} -AR expressed in INS-1E cells ($K_i=161.8$ nM). Radioligand experiments were normalized to % maximal binding. **(B)** Competition binding curves featuring increasing concentrations of bromocriptine using membranes prepared from HEK-293 cells transiently overexpressing α_{2A} -AR (in red) or D2R (in black) versus [3 H]-RX821002 or [3 H]-N-methylspiperone, respectively. Bromocriptine demonstrated 4.6-fold higher affinity for D2R ($K_i= 43.2$ nM) compared to α_{2A} -AR ($K_i= 198.7$ nM). Data represent mean \pm SEM performed in triplicate from $n=4$ independent experiments.

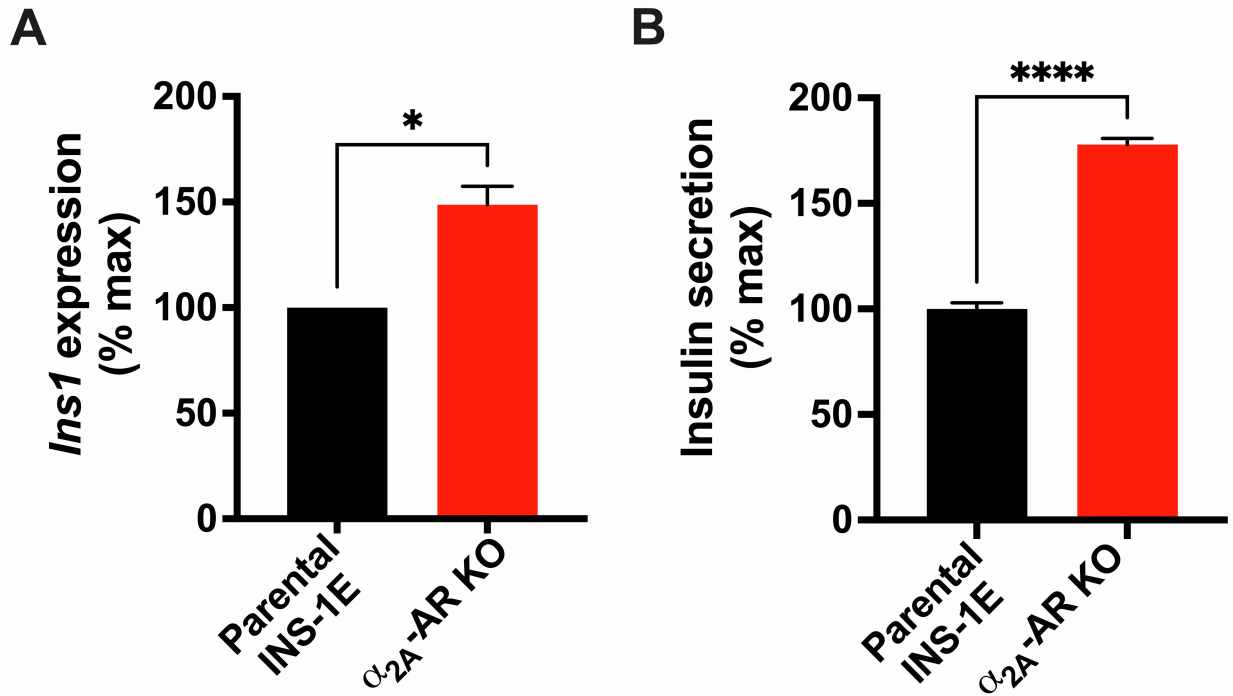


Figure S2. α_{2A} -AR KO upregulates *Ins1* expression and increases basal insulin secretion, related to Figure 1. (A) qPCR analysis comparing *Ins1* expression in α_{2A} -AR KO cells versus control parental INS-1E cells. *Ins1* mRNA expression was significantly upregulated in α_{2A} -AR KO cells (in red) compared to the parental INS-1E cells (in black; 48.8% increase, $p = 0.030$). Results were normalized to % *Ins1* expression in the parental INS-1E cells. Assays were independently performed on two separate experimental days. Data are represented as mean \pm SEM; two-tailed Student's t-test, * $p < 0.05$. **(B)** α_{2A} -AR KO cells (in red) demonstrated significantly enhanced basal insulin secretion in the absence of high glucose stimulation compared to the parental INS-1E cells (in black; 77.9% increase, $p < 0.0001$). Assays were performed in triplicate from $n \geq 3$ independent experiments. Insulin data were normalized to % maximal secreted insulin. Data are represented as mean \pm SEM; two-tailed Student's t-test, **** $p < 0.0001$.

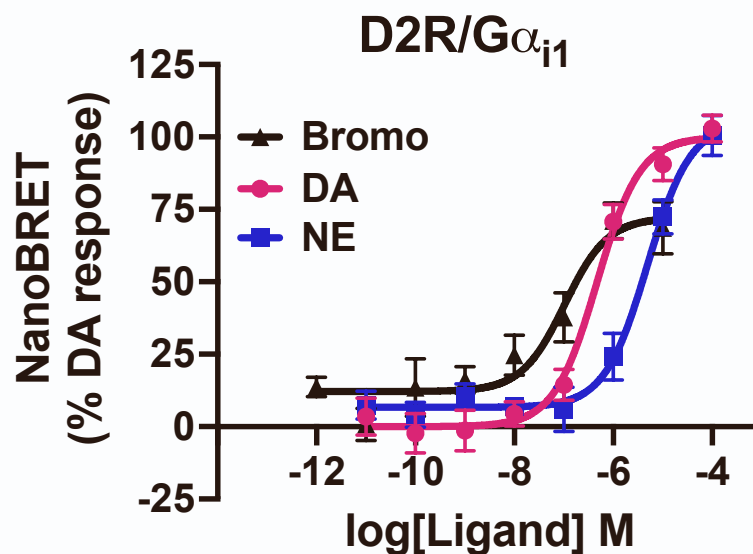


Figure S3. Bromocriptine stimulation of D2R results in G α_{i1} recruitment, related to Figure 4, Table 5, Table 6. Concentration-response nanoBRET assays examining drug-stimulated recruitment of Nano-Luc-labeled G α_{i1} in HEK-293T cells expressing HaloTag-labeled D2R. Cells were treated with either bromocriptine (in black), DA (in purple), or NE (in blue). Bromocriptine was more potent in recruiting G α_{i1} to D2R (EC_{50} =103.8 nM) compared to DA (EC_{50} =471.1 nM) or NE (EC_{50} =4897.5 nM), though with reduced efficacy versus these endogenous catecholamines (see **Tables 5, 6**). NanoBRET data were baseline-corrected and normalized to % maximal DA response. Assays were performed in triplicate from n=3 independent experiments. Data are represented as mean \pm SEM. NanoBRET data from DA and NE dose responses showing coupling of D2R with G α_{i1} were previously published in Aslanoglu et al., 2021.

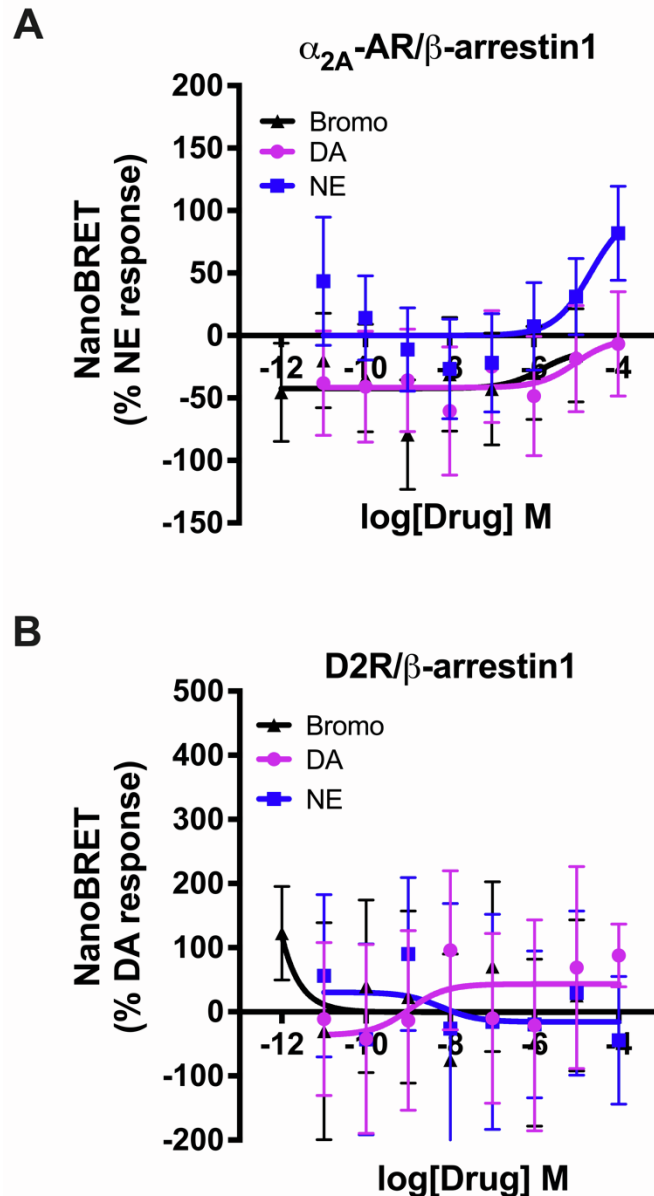


Figure S4. Bromocriptine stimulation results in negligible β -arrestin1 recruitment to D2R and α_{2A} -AR, related to Figure 5. Concentration response curves by nanoBRET examining ligand-stimulated recruitment of β -arrestin1 to D2R versus α_{2A} -AR. **(A)** Stimulation of α_{2A} -AR with either bromocriptine, DA, or NE caused only negligible β -arrestin1 receptor recruitment. **(B)** There was no significant dose-dependent β -arrestin2 recruitment to D2R in response to treatment with either bromocriptine, DA, or NE. NanoBRET data were baseline-corrected and normalized to either % maximal DA response for D2R or to % maximal NE response for α_{2A} -AR. Assays were performed in triplicate from $n \geq 3$ independent experiments. Data are represented as mean \pm SEM.

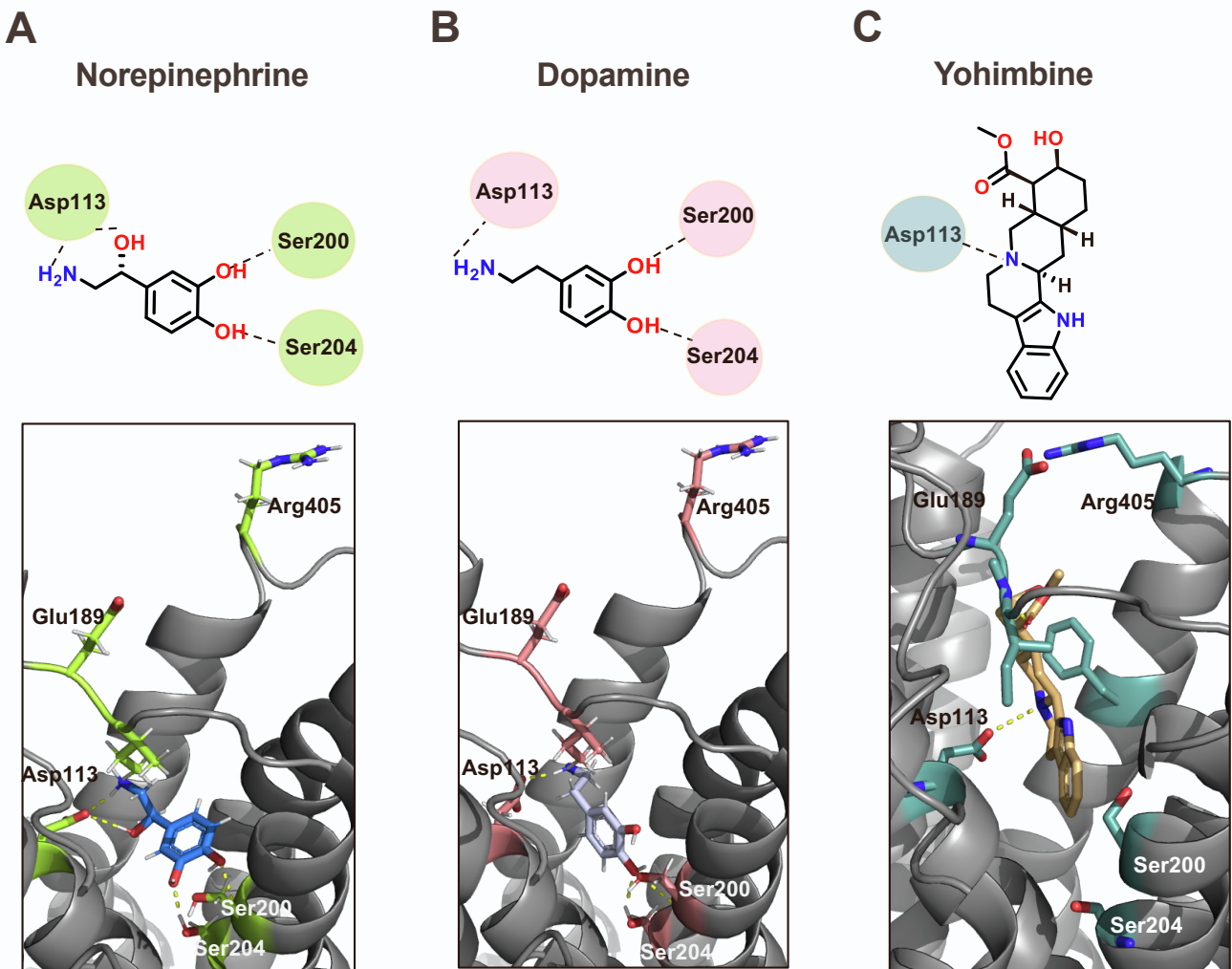


Figure S5. Predicted binding poses of ligands at α_{2A} -AR in two- and three-dimensions, related to Figure 6. Predicted binding poses of three α_{2A} -AR agonists: **(A)** NE, **(B)** DA and **(C)** α_{2A} -AR antagonist yohimbine using ROSETTALIGAND docking. Upper panels feature the respective two-dimensional views of ligand binding to α_{2A} -AR via docking and highlight key binding pocket residues. Lower panels show the predicted binding interactions in three-dimensional models with key amino acid residues highlighted within the α_{2A} -AR binding pocket.